7-2002

Preprogramming Of Porphyrin-nucleic Acid Assemblies Via Variation Of The Alkyl/aryl Substituents Of Phosphonium Tetratolylporphyrins

Pavel Kubat

Kamil Lang

Vladimir Kral

Pavel Anzenbacher Jr.
Bowling Green State University, pavel@bgsu.edu

Repository Citation

Preprogramming of Porphyrin−Nucleic Acid Assemblies via Variation of the Alkyl/Aryl Substituents of Phosphonium Tetratolylporphyrins

Pavel Kubát,[†] Kamil Lang,[‡] Vladimír Král,[§] and Pavel Anzenbacher, Jr.*[‖]

J. Heyrovský Institute of Physical Chemistry, Academy of Sciences of the Czech Republic, 182 23 Praha 8, Czech Republic, Institute of Inorganic Chemistry, Academy of Sciences of the Czech Republic, 250 68 Řež, Czech Republic, Institute of Chemical Technology at Prague, 166 28 Praha 6, Czech Republic, and Department of Chemistry and Center for Photochemical Sciences, Overman Hall, Bowling Green State University, Bowling Green, Ohio 43403

Cationic alkyl/arylphosphonium *meso*-tetratolylporphyrins aggregate in an aqueous solution to form H-aggregates, J-aggregates, and long-range assemblies. The ratio between the monomer and various types of aggregates can be controlled by the substitution in the phosphonium units and by the ionic strength. A trimethylphosphonium derivative is predominantly monomeric, dimethylphenylphosphonium forms monomers as well as low-molecular-weight H- and J-aggregates, triphenylphosphonium forms mainly H- and J-aggregates, and tri(*n*-butyl)phosphonium forms mainly long-range assemblies. Porphyrin monomers associate with calf thymus DNA (binding constant $K_b \approx 10^7$ M^{-1}) and oligonucleotides ($K_b \approx 10^5-10^6$ M^{-1}). The large size of the *meso*-substituents prevents the intercalation between base pairs. All phosphonium porphyrins described in this study were found to bind to the phosphate backbone of a nucleic acid with a significant preference for A−T base pair sequences. Porphyrin aggregates formed in the solution deposit readily on the surface of the DNA and oligonucleotides without changing their structure and size. Porphyrin monomers bound to DNA and nucleotides have photophysical properties (higher quantum yield of triplet states and singlet oxygen) different from those of porphyrin aggregates.

1. Introduction

Recognition processes involving nucleic acids are one of the most important features of living systems because they are a cornerstone of DNA replication and proteosynthesis.[1] Given the importance of the nucleic acids in the metabolism of a living organism, it is not surprising that nucleic acids are also among the most widely sought targets of numerous chemotherapeutics.[2] Water-soluble porphyrin derivatives have been the focus of numerous studies as potential therapeutic agents for the photodynamic therapy (PDT) of cancer[3] because of their antiviral activity,[4] and the ability to cleave selectively DNA[5] or RNA.[6] More recently, porphyrins were also utilized as tools in molecular biology applications such as DNA footprinting,[7] the design of telomerase inhibitors,[8] and stabilizing DNA/RNA hybrids,[9] DNA triplexes,[10] or DNA quadruplexes.[11] Likewise, the binding of porphyrins to DNA hairpins[12] and B-forms[13] or a specific sensing of DNA quadruplexes[14] has been recently described. The development in these areas is predicated upon a detailed understanding of the porphyrin−nucleic acid binding mechanism. Several different classes of positively charged porphyrins that show a strong ability to bind to DNA were investigated. These include derivatives bearing pyridinium and ammonium,[15,16] trialkylammonium,[17] guanidinium,[18] and quite recently also the trialkyl- and triarylphosphonium moieties.[19,20]

In general, three binding models have been described for the interaction of cationic porphyrins with DNA: (i) intercalation, (ii) outside groove binding, and (iii) outside binding with self-stacking. The latter mode leads to the formation of organized porphyrin structures on the DNA exterior.[21−24] Porphyrin derivatives, depending on their structure, and the presence of the coordinated metal including possible axial ligands, display different preferences not only for particular binding modes, but also for different DNA sequences. The investigations of the binding modes and sequence preferences have been performed using a wide variety of techniques such as X-ray crystallography, UV/vis, CD, fluorescence, RLS (resonance light scattering), and NMR spectroscopy experiments. It was found, for example, that cationic tetrakis(*N*-methylpyridinium-4-yl)porphyrin (TMPyP) and the corresponding planar metallocomplexes (e.g., Cu^{II}, Pd^{II}, Pt^{II}) possess the appropriate properties such as positive charge, hydrophobicity, appropriate size, and planar chromophore geometry favorable for intercalating between GC sites of DNA.[23,25] More sterically demanding porphyrins such as TMPyP metallocomplexes with axial ligands (ZnTMpyP, MnTMPyP, or CoTMPyP) or porphyrins with larger *meso*-substituents such as tetratolylporphyrin derivatives with ammonium and methylpyridyl groups[20] were found to bind to the DNA surface with a significant preference for A−T base pair rich sequences. This behavior is particularly pronounced in cationic tetratolylporphyrins bearing bulky phosphonium and sulfonium residues. These porphyrins show a strong tendency to form aggregates in aqueous solutions even at a concentration of 10^{-6}

* To whom correspondence should be addressed. Fax: (419) 372 9809. Phone: (419) 372 2080. E-mail: pavel@bgnet.bgsu.edu.
† J. Heyrovský Institute of Physical Chemistry, Academy of Sciences of the Czech Republic. E-mail: kubat@jh-inst.cas.cz.
‡ Institute of Inorganic Chemistry, Academy of Sciences of the Czech Republic. E-mail: lang@ iic.cas.cz.
§ Institute of Chemical Technology at Prague. E-mail: vladimir.kral@ vscht.cz.
‖ Bowling Green State University.

Preprogramming of Porphyrin−Nucleic Acid Assemblies

J. Phys. Chem. B, Vol. 106, No. 26, 2002 **6785**

M and bind to DNA mainly in the form of an aggregate.[19,20] The Soret band position for cofacial aggregates (H-aggregate) is blue-shifted, whereas for the side-by-side aggregates (J-aggregates) it is red-shifted. Estimates based on RLS suggest the size of these aggregates to be between 15 and 27 Å. The aggregation processes are very important because they have a dramatic effect on the photochemical behavior of porphyrins. For example, the fluorescence quantum yields of porphyrin aggregates are at least more than 1 order of magnitude lower than those of the corresponding monomeric free-base porphyrins.[26] The aggregation has, therefore, an enormous impact on the ability of porphyrins to effect photosensitization and cleavage of nucleic acids. The latter process occurs by a photoinduced mechanism involving either the porphyrin excited singlet and triplet states or singlet oxygen, and leads to oxidative attack of a sugar moiety and strand scission.[27] The aggregation behavior of porphyrin derivatives has to be taken into account in the application of porphyrins, as well as in the design of the porphyrin sensitizers for an application in the PDT of cancer in particular.

In this study, we describe the synthesis of alkyl/arylphosphonium tetratolylporphyrins and their aggregation behavior in solution and in the presence of DNA and DNA oligonucleotides. It is important to note that the phosphonium groups in porphyrins P_1-P_4 are insulated from the porphyrin ring by a methylene bridge and thus have a minimal influence on the electron density in the π-system of the porphyrin chromophore.[28] We have synthesized a group of porphyrin derivatives that encompass the full range of the aggregation behavior, and have investigated the relationship between the chemical structure and the aggregation behavior. It is shown here that the variation of alkyl/aryl substituents of the phosphonium group can be used to effectively control the nature of the DNA−porphyrin complexes.

2. Experimental Section

A. Materials and General Methods. Solvents and other reagents for synthesis were purchased from Aldrich Chemical Co. Tetrahydrofuran and toluene were distilled in the presence of potassium metal. Anhydrous methanol was obtained by distillation from magnesium metal. NMR spectra were recorded on Varian Unity 300 MHz and Varian Unity Plus 400 MHz spectrometers using the solvent as reference. NMR shifts (δ) are reported in parts per million; coupling constants are reported in hertz. Elemental analyses were performed on a Perkin-Elmer 240 (ICT) instrument. Mass spectra were recorded on ZAB-EQ and ZAB SEQ VG Analytical spectrometers.

Adenosine 5′-monophosphate (AMP), guanosine 5′-monophosphate (GMP), cytidine 5′-monophosphate (CMP), and thymidine 5′-monophosphate (dTMP) were obtained as sodium salts from Sigma and used without further purification. The oligonucleotides 5′-A_8-3′, 5′-G_8-3′, 5′-C_8-3′, 5′-T_8-3′, 5′-G_{16}-3′, and 5′-C_{16}-3′ (abbreviated for simplicity as A_8, G_8, C_8, T_8, G_{16}, and C_{16}) were purchased from Generi Biotech (Czech Republic). The double-stranded oligonucleotides (e.g., G_8C_8) were prepared from the corresponding oligonucleotides by mixing their buffered solutions. The molar concentration of oligonucleotides, single- or double-stranded, was quantified by UV spectroscopy. The concentration of calf thymus double-stranded DNA from Sigma (DNA), calculated in base pairs, was determined spectrophotometrically using molar absorptivity $\epsilon_{260} = 1.31 \times 10^4$ M^{-1} cm^{-1} according to the literature.[29] Stock solutions of the porphyrins (ca. 200 μM) were prepared in methanol (Riedel-de Haën, HPLC grade) and stored in the dark. Stock solutions were diluted with water, phosphate buffer, or methanol prior to use.

B. Synthesis of Porphyrin Materials. 5,10,15,20-Tetrakis-(α-bromo-*p*-tolyl)porphyrin (P_0),[30] 5,10,15,20-tetrakis(α-triphenylphosphonio-*p*-tolyl)porphyrin tetrabromide salt (P_3), and 5,10,15,20-tetrakis(α-tri-*n*-butylphosphonio-*p*-tolyl)porphyrin tetrabromide salt (P_4) were prepared according to the previously published procedures.[20] The identical method was adopted to prepare novel porphyrins P_1 and P_2 described in this paper.

5,10,15,20-Tetrakis(α-[trimethylphosphonium]-p-tolyl)porphyrin tetrabromide salt (P_1) was prepared by heating porphyrin P_0 (0.987 g, 1.0 mmol) with a 10-molar excess of trimethylphosphine in a deoxygenated methanol−tetrahydrofuran (THF) (2:1) mixture (50 mL) in a sealed vessel to 80 °C for 24 h under argon. The reaction mixture was evaporated in vacuo, and the residue was thoroughly washed with hot THF on the frit. Further purification was performed by dissolving the solid in hot water with addition of THF to promote crystallization. The yield was 1.100 g (85%).

^{1}H NMR (DMSO-d_6): δ −2.95 (br s, 2H, pyrrole NH), 2.50 (d, 24H, J = 14.4 Hz, PCH$_3$), 4.23 (d, 8H, J = 16.8 Hz, CH$_2$P), 7.78 (m, 8H, aromatic CH), 8.27 (m, 8H, aromatic CH), 8.92 (s, 8H, β-pyrrole CH).

^{13}C NMR (DMSO-d_6): δ 7.3 (d, J = 53.9 Hz), 29.4 (d, J = 47.1 Hz), 119.5, 127.4, 128.5 (d, J = 6.9 Hz), 129.5 (d, J = 9.1 Hz), 137.9, 140.6 (d, J = 4.6 Hz), 141.1.

MS/FAB+ (*m/z*): 1208.3 [M − Br].

Anal. Calcd for $C_{60}H_{70}Br_4N_4P_4$: C, 55.83; H, 5.47; N, 4.34. Found: C, 55.69; H, 5.51; N, 4.31.

UV/vis (MeOH) [λ, nm (ϵ, 10^{-4} M^{-1} cm^{-1})]: 415 (30), 513 (1.4), 547 (0.71), 589 (0.50), 645 (0.37). Fluorescence (MeOH) (λ, nm): 654, 719.

5,10,15,20-Tetrakis(α-[dimethylphenylphosphonium]-p-tolyl)-porphyrin tetrabromide salt (P_2) was prepared by heating P_0 (0.987 g, 1.0 mmol) with a 10-molar excess of dimethylphenylphosphine in a deoxygenated methanol−THF (2:1) mixture (50 mL) in a sealed vessel to 80 °C for 24 h under argon. The volume of the reaction mixture was reduced in vacuo to 15 mL, and the porphyrin material was precipitated by addition of THF. The precipitate was thoroughly washed with hot THF on the frit. Further purification was performed by dissolving the solid in a hot water−methanol (1:1) mixture with addition of THF to promote crystallization. The yield of dark violet microcrystals was 1.216 g (79%).

^{1}H NMR (DMSO-d_6): δ −2.98 (br s, 2H, pyrrole NH), 2.50 (d, 24H, J = 14.5 Hz, PCH$_3$), 4.49 (d, 8H, J = 19.7 Hz, CH$_2$P), 7.51−7.58 (m, 6H, aromatic CH), 7.79−7.90 (m, 12H, aromatic CH), 8.00−8.22 (m, 18H, aromatic CH) 8.82 (s, 8H, β-pyrrole CH).

^{13}C NMR (DMSO-d_6): δ 6.3 (d, J = 53.9 Hz), 30.6 (d, J = 47.7 Hz), 119.4 (d, J = 9.1 Hz), 120.2 (d, J = 12.2 Hz), 121.1 (d, J = 12.2 Hz), 127.9, 128.5, 129.0 (d, J = 9.1 Hz), 129.4 (d, J = 12.2 Hz), 132.1 (d, J = 9.9 Hz), 134.3, 134.6, 137.9, 140.6, 141.0.

MS/FAB+ (*m/z*): 1457.2 [M − Br].

Anal. Calcd for $C_{80}H_{78}Br_4N_4P_4$: C, 62.43; H, 5.11; N, 3.64. Found: C, 62.29; H, 5.03; N, 3.56.

UV/vis (MeOH) [λ, nm (ϵ, 10^{-4} M^{-1} cm^{-1})]: 416 (48), 514 (2.1), 548 (1.0), 589 (0.63), 645 (0.46). Fluorescence (MeOH) (λ, nm): 654, 719.

C. Spectroscopic Methods. All absorption spectra were recorded using a Perkin-Elmer Lambda 19 spectrophotometer. Absorption spectra of P_1-P_4 were monitored as a function of nucleic acid concentration in 20 mM phosphate buffer (pH 7.0) in the presence of 0−100 mM NaCl. Absorbance titrations were performed by adding concentrated stock solutions of nucleotides

(up to 100 mM), oligonucleotides (up to 0.50 mM), or DNA (up to 3 mM in base pairs) to the porphyrin solution. The concentration of the porphyrin solutions was between 1.0 and 2.7 μM. All measurements were corrected for a dilution caused by the volume of added solution (<30%). After each addition the cell was kept at room temperature (25 °C) for 5 min for equilibration. In the case of DNA, the experiments were performed at different porphyrin/DNA base pair molar concentration ratios R. Binding stoichiometries of the $\mathbf{P}_1$ adducts were obtained by Job's method of continuous variations. The solutions of porphyrin and oligonucleotide were mixed to a standard volume while the sum of both concentrations was kept constant at 3 μM. Two sets of solutions with the same $\mathbf{P}_1$ concentrations were prepared in the presence and absence of oligonucleotide. Absorbance differences were recorded at 421 nm. The binding stoichiometry was obtained from the intercepts after linear least-squares fits to the left- and right-hand portions of the Job plots.

Binding of $\mathbf{P}_1$ with nucleotides was performed in 20 mM phosphate buffer. Because of the high nucleotide concentrations (up to 100 mM), the ionic strength was not controlled by NaCl. The binding constants K_b for $\mathbf{P}_1$–nucleotide adducts were determined using the Benesi–Hildebrand equation assuming a 1:1 stoichiometry (eq 1).[31] In eq 1, ΔA is the difference in

$$\frac{1}{\Delta A} = \frac{1}{K_b c_N (\Delta A)_\infty} + \frac{1}{(\Delta A)_\infty} \qquad (1)$$

absorbance of the porphyrin solution in the presence and absence of the nucleotide at the Soret maximum, $(\Delta A)_\infty$ represents the extrapolated absorbance change at infinite nucleotide concentration, and the concentration of added nucleotide c_N is always significantly larger than the concentration of $\mathbf{P}_1$.

The component resolution of the observed $\mathbf{P}_1$ spectra in the presence of oligonucleotides was performed using a linear multiple regression.[32] Using the known molar absorption coefficients of both free and bound $\mathbf{P}_1$ in the Soret region, we have calculated equilibrium concentrations of both species at a given concentration of oligonucleotide. The obtained data were used to calculate the binding constant for a 1:1 adduct as confirmed by Job plot calculations. Similarly, the absorption spectra of $\mathbf{P}_1$–oligonucleotide complexes were also treated using the Scatchard equation (eq 2). In eq 2, r is the ratio of the molar

$$r/c_F = K_b(n - r) \qquad (2)$$

concentration of bound $\mathbf{P}_1$ to that of oligonucleotide, c_F is the concentration of free (unbound) $\mathbf{P}_1$, K_b is the binding constant of the $\mathbf{P}_1$–oligonucleotide adduct, and n is the number of identical binding sites for $\mathbf{P}_1$.

Binding data for $\mathbf{P}_1$ to DNA were analyzed by a neighbor exclusion model suggested by McGhee and von Hippel (eq 3).[33]

$$\frac{r}{c_F} = K_b(1 - mr)\left[\frac{1 - mr}{1 - (m - 1)r}\right]^{m-1} \qquad (3)$$

In eq 3, m is the exclusion parameter expressed in base pairs, which describes the number of potential binding sites removed by a binding event. The values of r and c_F were calculated from absorption spectra assuming the $\mathbf{P}_1$ is completely bound at a 50-fold excess of DNA. Molar concentrations of DNA are expressed in base pairs.

Steady-state fluorescence spectra were recorded using a Perkin-Elmer LS 50B luminescence spectrophotometer. All fluorescence spectra were corrected for the characteristics of the detection monochromator and photomultiplier using a
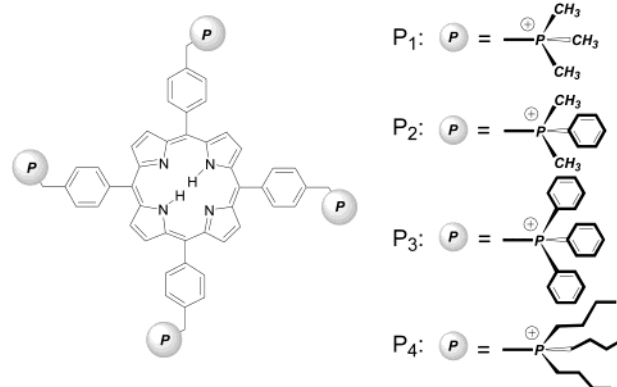

Figure 1. Structures of *meso*-tolylporphyrins with alkyl- and arylphosphonium groups.

recently described procedure.[34] The samples were excited at the $Q_y(1,0)$ absorption band around 520 nm because this band is less influenced by binding than the Soret band. The fluorescence quantum yields were obtained by a comparison of the integrated area under the emission spectra of the $\mathbf{P}_1$ samples with 5,10,15,20-tetrakis(4-sulfonatophenyl)porphyrin ($\Phi_f = 0.060 \pm 0.005$).[35] The absorbances were adjusted to the same value at the excitation wavelength (<0.08/1 cm cell). All experiments were performed in air-saturated 20 mM phosphate buffer (pH 7.0) at room temperature.

RLS experiments were conducted using simultaneous scans of the excitation and emission monochromators through the range of 300–600 nm on a Perkin-Elmer LS 50B luminescence spectrophotometer.

The circular dichroism (CD) spectra were recorded using a Jobin Yvon-Spex CD 6 spectrometer. The spectra at selected porphyrin/DNA concentration ratios R were obtained by averaging three accumulations recorded with steps of 0.5 nm and an integration time of 1s.

Laser flash photolysis experiments were performed with a Lambda Physik FL 3002 dye laser (414–424 nm, output 0.05–5 mJ/pulse, pulse width ~28 ns). Transient spectra were recorded within 300–600 nm on a laser kinetic spectrometer (Applied Photophysics, U.K.). The time profiles of the triplet-state decay were recorded at 450 nm using a 250 W Xe lamp equipped with a pulse unit and a R928 photomultiplier (Hamamatsu). Time-resolved near-infrared emission of singlet oxygen $O_2(^1\Delta_g)$ at 1270 nm was observed at the right angle to the excitation light using a detector unit built by us (interference filter, Ge diode Judson J16-8SP-R05M-HS).

3. Results and Discussion

A. Design of Porphyrin Derivatives. Our previous reports[20,36] reveal that almost all of the alkyl/arylphosphonium-substituted porphyrins show a pronounced aggregation in aqueous solutions. Here, we report on the synthesis of the porphyrin derivatives $\mathbf{P}_1$ and $\mathbf{P}_2$ designed to complete the series of previously described phosphonium porphyrins for additional derivatives that show a distinct tendency toward a monomeric state ($\mathbf{P}_1$) as well as the equilibrium of monomer and aggregated states ($\mathbf{P}_2$).

It is important to note that even relatively small changes in the character of the alkyl substituents of the phosphonium moieties indeed do have a crucial impact on the aggregation behavior as well as the nature of the porphyrin assemblies deposited on the surface of the oligonucleotide material or DNA. Figure 1 shows phosphonium porphyrins described in this study: 5,10,15,20-tetrakis(α-trimethylphosphonium-*p*-tolyl)por-

Preprogramming of Porphyrin−Nucleic Acid Assemblies
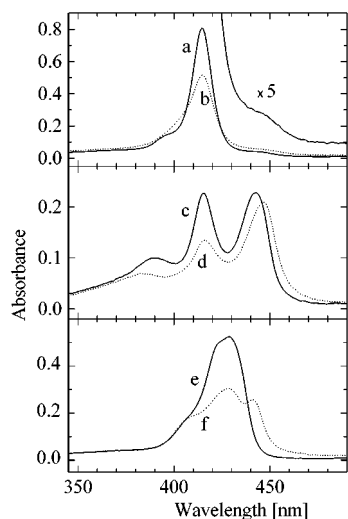
J. Phys. Chem. B, Vol. 106, No. 26, 2002 **6787**

Figure 2. Effect of porphyrin hydrophobicity and ionic strength on the aggregation behavior recorded in 20 mM phosphate buffer (pH 7.0). Soret bands of porphyrins: 2.7 μM P_1 (5× magnified trace a), 2.7 μM P_1 in the presence of 1.4 M NaCl (b), 1.6 μM P_2 (c), 1.6 μM P_2 in the presence of 0.8 M NaCl (d), 2.2 μM P_3 (e), 2.2 μM P_3 in the presence of 0.6 M NaCl (f).

phyrin (P_1), 5,10,15,20-tetrakis(α-dimethylphenylphosphonium-*p*-tolyl)porphyrin (P_2), 5,10,15,20-tetrakis(α-triphenylphosphonio-*p*-tolyl)porphyrin (P_3), and 5,10,15,20-tetrakis(α-tri-*n*-butyl-phosphonio-*p*-tolyl)porphyrin (P_4), all in the form of their respective tetrabromide salt.

B. Porphyrin Aggregates in Aqueous Solutions. To understand the nature of complexation between porphyrins and nucleic acids, a detailed understanding of the porphyrin behavior in aqueous electrolyte solutions is required. Porphyrins P_1−P_4 (Figure 1) show typical monomeric spectra in methanol with a Soret band at 415−416 nm, and four Q-bands at longer wavelengths. The absorption spectra of methanolic solutions were found to be in accord with the Lambert−Beer law at concentrations up to 10^{-5} M. All P_1−P_4 are well soluble in water with some degree of aggregation as indicated by a broadening of the Soret bands (Figure 2) as well as by deviations from the Lambert−Beer law. The presence of large porphyrin aggregates in water was confirmed by RLS measurements, which is a sensitive method for obtaining detailed information about extended aggregates including the absorption spectrum and the average size of the scattering species.[37,38] It should be noted that the porphyrin monomers and small aggregates do not show resonance light-scattering profiles. The association of π-conjugated porphyrin rings is regarded as a combination of attractive σ−π and repulsive π−π interactions.[39]

The absorption spectra of P_1 follow the Lambert−Beer law up to 10 μM concentration at a relatively high ionic strength ($\leq$0.3 M NaCl). The presence of the low-intensity shoulder at about 450 nm suggests a small contribution of the aggregated species (<5%, Figure 2a) that is confirmed by a low-intensity RLS peak. P_1 is the first example of cationic phosphonium porphyrin known to be predominantly monomeric in aqueous solutions. However, at high ionic strength ($\geq$1.4 M NaCl) a certain broadening and hypochromicity of the Soret band indicating aggregation was observed (Figure 2b). In contradistinction to P_1, a substitution of one of the methyl groups of the phosphonium substituents with a phenyl residue in P_2 resulted in a higher tendency to form aggregates. This behavior is reflected by a marked broadening and a splitting of the Soret band into three individual bands located at 389, 414, and 443 nm, respectively (Figure 2c,d). Here the band centered at 414
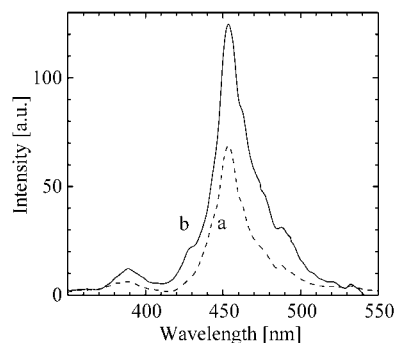

Figure 3. Resonance light-scattering spectra of 1.5 μM P_2 in the absence of DNA (a) and in the presence of DNA ($R = 0.550$) (b) (20 mM phosphate buffer, pH 6.9, 100 mM NaCl).

nm was unequivocally ascribed to the monomer of P_2. For comparison, in methanol the same band is located at 416 nm. These features are in agreement with the exciton theory, which predicts that the excited-state energy level of a monomeric dye splits into two upon aggregation, and that the shift of the transition to the higher states depends on the structure of the aggregated species.[40] While the presence of the blue-shifted band at 389 nm indicates the formation of sandwich-type aggregates (H-aggregate), the red shift of the Soret band to 443 nm is attributed to a side-by-side aggregation and a formation of J-aggregates. In the case of P_2, the presence of a variety of contributing structures explains why the band corresponding to the J-aggregate is relatively broad. The J-aggregates of P_2 are connected with the emergence of a light-scattering band at 454 nm (Figure 3a).

The porphyrin P_3 with all three methyl groups replaced by phenyl moieties shows an unresolved Soret band which, upon increased ionic strength, shows a certain tendency toward resolution into three bands centered at 408, 427, and 443 nm, respectively (Figure 2e,f), corresponding to various types of aggregates. Similarly to P_3, in porphyrin P_4 the presence of the three hydrophobic *n*-butyl groups attached to the phosphorus atom causes extensive aggregation even in distilled water. The Soret band is unresolved and broad (not shown).

In general, a high ionic strength causes a gradual decrease of the monomer absorption bands together with the increase of the light-scattering profiles, indicative of extensive aggregation. The degree of aggregation for P_1−P_4 depends strongly on the number and the type (alkyl/aryl) of the phosphonium group substituents. Only P_1 displays monomeric behavior in aqueous solutions even at high ionic strength. The porphyrin P_2 exhibits the presence of both monomers and aggregates, while the porphyrins P_3 and P_4 form predominantly aggregates. The observed tendency to form aggregates at the same ionic strength increases in the order $P_1 \ll P_2 \ll P_3 < P_4$. The aggregation properties of the reported porphyrins have a major impact on the formation of porphyrin−oligonucleotide/DNA complexes, as shown in the following paragraphs.

C. Binding of the Porphyrin Monomer to Nucleotide Monophosphates. The first insight into the binding capabilities of P_1 was obtained from the investigation of the interaction between P_1 and individual nucleotide monophosphates. During UV/vis titration the Soret band of P_1 at 414 nm is bathochromically shifted, and a single isosbestic point indicates the formation of a well-defined complex. The Benesi−Hildebrant analysis gives excellent fits assuming a 1:1 stoichiometry for the complexes. The resulting values of the binding constants K_b are presented in Table 1. The binding constants are larger for purine bases (A, G) than pyrimidines (C, T). Double-ring

TABLE 1: Porphyrin P₁ Bound to Mononucleotides, Oligonucleotides, and DNA in 20 mM Phosphate Buffer (pH 7.0, 100 mM NaCl) at Room Temperature (25 °C): Molar Absorption Coefficients (ϵ_b) at the Soret Maximum (λ_{max}), Binding Constants [K_b (M⁻¹)] Obtained by Titration of 1.7 μM P₁, Fluorescence Quantum Yields (Φ_f), Fluorescence Emission Bands (λ_f), and Quenching Rate Constants of the Triplet States of Bound P₁ by Oxygen (k_T) in Air-Saturated Solutions

	absorption			fluorescence		triplet states
ligand	λ_{max} (nm)	ϵ_b (10^{-5} M⁻¹)	binding $K_b{}^a$ (M⁻¹)	λ_f (nm)	$\Phi_f{}^a$	$k_T{}^{a,b}$ (10^{-4} s⁻¹)
	414	2.8		651, 709	0.051	60
AMP	421^c	2.1^c	230^d			35
GMP	420^c	2.0^c	450^d	658, 720	0.048	36
dTMP	418^c	2.3^c	130^d			31
CMP	417^c	2.1^c	15^d	656, 714		53
G₈	422	1.6	$3.6 \times 10^{5\,e}$			
C₈	421	1.9	$4.9 \times 10^{5\,e}$	657, 721	0.047	
G₈C₈	421	1.7	$1.4 \times 10^{6\,e}$			9.7
G₁₆C₁₆	424	1.8	$2.4 \times 10^{6\,e}$	660, 722	0.046	6.8
T₈	422	2.3	$3.9 \times 10^{6\,e}$	657, 722	0.044	7.6
A₈T₈	422	2.0	$7.3 \times 10^{6\,e}$	657, 721	0.047	7.9
A₁₆T₁₆	422	1.7	2.1×10^6 (3.6 ± 0.5)^f			7.4
DNA	421	1.9	1.0×10^7 (8.6 ± 0.7)^g	655, 720	0.036^h	7.2

^{a} The estimated error from independent experiments was less than 15%. ^{b} The triplet states were recorded at 450 nm. In some cases we observed biexponential fits due to the presence of both bound and free P₁. The rate constant k_T of free P₁ was fixed at 6.0×10^5 s⁻¹. ^{c} Measured for 0.1 M nucleotides in 20 mM phosphate buffer. ^{d} Calculated using the Benesi−Hildebrand equation assuming a 1:1 complex. ^{e} Calculated using linear multiple regression.[32] ^{f} Calculated using the Scatchard equation; the number of identical but independent binding sites is in parentheses. ^{g} McGhee−von Hippel neighbor exclusion model: the DNA concentration is in base pairs; the number of base pairs (potential binding sites) removed by P₁ is in parentheses. ^{h} Fluorescence data for $R = 0.057$.

structures of purines (A, G) give rise to stronger van der Waals interactions and more extensively perturb the electron configuration of the porphyrin than pyrimidines (C, T). The pronounced interactions are reflected by the increased values of binding constants as well as larger bathochromic shifts of the Soret bands (3−7 nm) in P₁−AMP or P₁−GMP complexes. The calculated values of binding constants K_b are, however, almost 1 order of magnitude lower than those measured for TMPyP.[41,42] This feature is understood as a result of the pronounced steric hindrance caused by the alkyl/aryl residues attached to the phosphorus atom, thus rendering the positive charge less accessible for the nucleotide anion.

D. Binding of the Porphyrin Monomer to Oligonucleotides and DNA. The phosphonium porphyrins P₁−P₄ show a strong tendency to form complexes with oligonucleotides and DNA on the basis of the electrostatic attraction between the positive charges of the phosphonium moieties and the negatively charged backbone of the oligonucleotide/DNA. All experimental data including absorption, fluorescence, and CD spectroscopy experiments indicate an outside binding mode. Specifically, the small red shift with relatively small hypochromicity of the Soret band and a positive CD signal are, in fact, a hallmark of the outside binding of the porphyrin units without stacking on the nucleic acid surface.[43]

The binding of P₁ to single- and double-stranded oligonucleotides was examined by UV/vis and fluorescence spectroscopy. The molar absorption coefficients of the Soret bands show a more than 30% decrease, and the band positions shift toward longer wavelengths by 7−10 nm (Figure 4a,c). The red shift of the Soret band is accompanied by a shift of the fluorescence emission bands (Figure 4b,d) as well as a decrease in the fluorescence quantum yields Φ_f. The resolution of the Q(0,0) and Q(0,1) fluorescence emission bands becomes more apparent and shows a distinct similarity to those of the emission spectra in less polar solvents such as methanol. The fluorescence properties of the complexes appear to be independent of oligonucleotide structure including DNA. Figure 4 and the data in Table 1 present the spectral changes of P₁ upon addition of oligonucleotides and DNA. The overall binding stoichiometry of P₁ to single- and double-stranded oligonucleotides was examined by the method of continuous variation. The Job plot
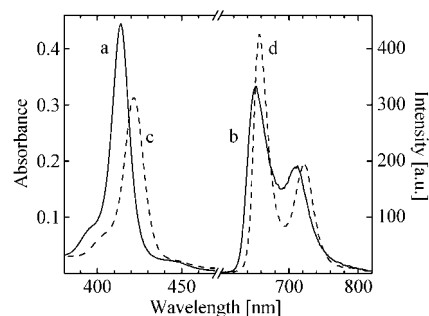

Figure 4. UV/Vis (a, left axis) and fluorescence emission (b, right axis) spectra of 2.7 μM P₁ in comparison with UV/vis (c, left axis) and fluorescence emission (d, right axis) spectra of the 1:1 adduct P₁−A₈T₈ (20 mM phosphate buffer, pH 7.0, 100 mM NaCl, 47 μM A₈T₈). Fluorescence spectra were recorded using optically matched solutions at an excitation wavelength of 518 nm ($A_{518} = 0.042$/1 cm cell).
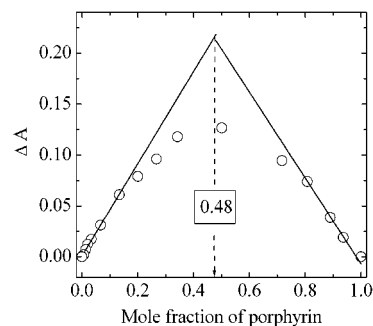

Figure 5. Job plot for binding of P₁ to C₈ in 20 mM phosphate buffer (pH 7.0, 100 mM NaCl). The value of ΔA represents the difference in the absorbances for P₁ in the presence of C₈ and in buffer alone at 421 nm.

for C₈ is shown in Figure 5. The observed intercept of 0.48 indicates that the stoichiometry of the complex between P₁ and C₈ is 1:1. This value was also found for other oligonucleotides (Table 1). The only exception is double-stranded A₁₆T₁₆ containing 3−4 equivalent binding sites. The comparison of the binding constants suggests that P₁ exhibits a more than 3 orders of magnitude increase of affinity to nucleic acids over nucleotide monophosphates. This is most likely caused by multiple
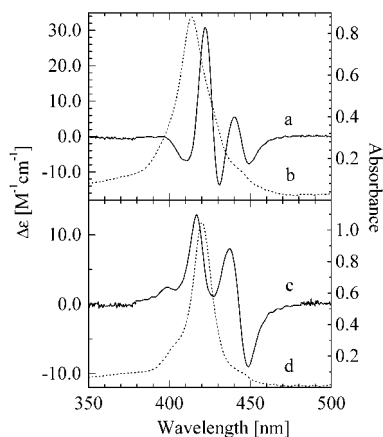
Preprogramming of Porphyrin−Nucleic Acid Assemblies

J. Phys. Chem. B, Vol. 106, No. 26, 2002 **6789**

Figure 6. Induced circular dichrism spectra of 5.4 μM P_1 by DNA at $R = 1.06$ (a) and $R = 0.036$ (c) with corresponding absorption spectra (right axis) (b, d) (20 mM phosphate buffer, pH 7.1, 10 mM NaCl).

Figure 7. Fluorescence emission spectra of 2.7 μM P_1 in the absence of C_8 ($A_{271 nm} = 0.032/1$ cm cell) (a) and in the presence of 3.9 μM C_8 ($A_{271 nm} = 0.219/1$ cm cell) (b) (excitation wavelength 271 nm, 20 mM phosphate buffer, pH 7.1, no NaCl present in order to increase the adduct concentration).

Coulombic interactions between phosphonium moieties and phosphates of the oligonucleotide backbone. The binding constants of P_1 toward single-stranded G_8 and C_8 are similar. The affinity toward double helices of G_8C_8 increases more than the simple sum of the respective K_b for single strands. However, affinity toward single-stranded T_8 appears to be even higher than that of the G_8C_8 duplex. The duplex A_8T_8 exhibits the highest value of K_b from all studied oligonucleotides.

The final confirmation of the successful design of P_1 came from the binding experiments with DNA. The spectroscopic behavior of P_1 is sensitive to the molar ratio of porphyrin to DNA (R) and to the ionic strength adjusted by NaCl. For example, when 2.7 μM P_1 in 10 mM NaCl is titrated (R is decreasing), the absorption spectra exhibit an isosbestic point at 421 nm. However, it shifts to 414 nm when R becomes lower than 0.310. In 50 mM NaCl we observed a shift of the isosbestic point from 420 to 416 nm for $R < 0.225$. Moreover, at high R (R close to 1), the Soret band is significantly broadened (compare Figure 6b,d) and the intensity of light-scattering profiles at about 450 nm increases 3 times compared with those of solutions of P_1 in the absence of DNA. These results suggest that at high R the monomer of P_1 saturates the DNA surface and continues to deposit a creating layer of various aggregated species and extended porphyrin assemblies. Upon further addition of the DNA ($R \ll 1$), the extended porphyrin assemblies disassemble to a rather uniform P_1−DNA complex in which P_1 is spread on the DNA surface as a monomer (the preferred state). Unlike in the 50 mM NaCl solution, in the 100 mM NaCl solution, we observed only one isosbestic point at 418−419 nm. The observed spectral features are typical for equilibrium between the bound monomer and a free porphyrin monomer in solution. Evidently, the competitive effect of a high ion concentration renders the assembling of P_1 on the DNA surface ineffective. These conclusions are supported by CD spectra (Figure 6) as well as fluorescence resonance energy transfer (Figure 7).

At equimolar concentrations ($R \approx 1$) the CD spectrum reveals a dominant bisignate signal with a positive band at 422 nm ($\Delta\epsilon = 31.1$ M^{-1} cm^{-1}) (Figure 6a) and a conservative signal with a zero point at 444 nm. This conservative signal was found in all spectra regardless of R and can be attributed to extended porphyrin assemblies formed by the binding of an achiral aggregate present in a small amount in the solution (small absorption and RLS around 450 nm; see section 3B) to the chiral DNA backbone. At $R < 0.05$ the spectrum shows a positive CD band at 417 nm ($\Delta\epsilon = 13$ M^{-1} cm^{-1}) together with
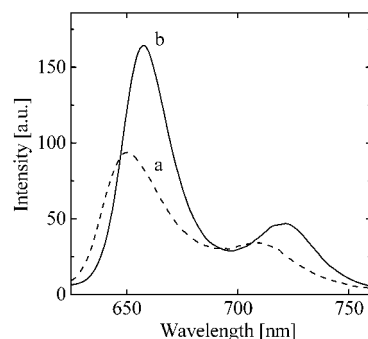
conservative features with a zero point at 443 nm (Figure 6c). At $R = 0.2$, the position of the positive 417 nm band is red-shifted to 424 nm (only a shoulder is observed at 417 nm) while its intensity remains constant. In the experiment carried out at $R = 0.036$, both the positive band at 417 nm and, similarly, the positive band centered at 424 nm were assigned to a monodispersed porphyrin in two different binding sites, which agreed with literature results.[20] The high-intensity bisignate signal at $R \approx 1$ most likely consists of several overlapping features, rendering the resolution into the respective contributions difficult. These observations confirm our conclusion derived from the UV/vis and RLS spectra that porphyrin assembling takes place at high R even at low ionic strength. The interval of R at which the porphyrin P_1 is bound predominantly as a monomer (monodispersed porphyrin) is limited by the ionic strength. This process occurs with all studied nucleic acids regardless of their sequence. In summary, the increased concentration of nucleic acids reduces the driving force for the porphyrin compaction.

Fluorescence resonance energy transfer (FRET) occurs when energy absorbed by a fluorescent donor is transferred to an acceptor molecule in the ground state. The extent of energy transfer depends on the distance between the donor and the acceptor and their spectral properties and mutual orientation. FRET is therefore an ideal method to investigate the porphyrin−DNA interactions.[44] To investigate the possibility of energy transfer from oligonucleotides or DNA (a donor) to porphyrin (acceptor), a set of fluorescence excitation and emission experiments were run with either free P_1 or P_1 bound to oligonucleotide. Figure 7 shows that the binding of P_1 to C_8 leads to a clear increase of the porphyrin fluorescence quantum yields by a factor of approximately 1.4 after excitation at the nucleic acid band (271 nm) compared with that of the free porphyrin (Figure 7a,b), even though Φ_f of the complex is generally lower than that of free P_1 (Table 1). This proves that light absorbed by the oligonucleotide is transferred to P_1. This effect is explained by the binding of P_1 to oligonucleotides, single- or double-stranded nucleic acids from Table 1, which drives both the porphyrin and the nucleobase together into an effective distance and orientation for FRET to occur. Under identical conditions, we did not observe energy transfer to the bound P_2 due to a considerable quenching of its fluorescence, a result of self-stacking on the nucleic acid surface (see below).[45]

The binding of P_1 to DNA falls into the category of relatively strong interactions compared to that of other tetratolyl-type porphyrins bearing positively charged substituents.[20] The UV/vis and CD spectral data unambiguously confirm binding of the P_1 monomer to the outer surface of DNA characterized by a binding constant K_b of 1.0×10^7 M^{-1}. Similarly to other
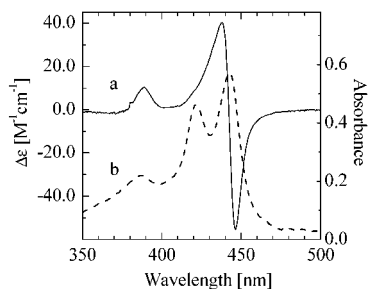
6790 *J. Phys. Chem. B, Vol. 106, No. 26, 2002*

Kubát et al.

Figure 8. Induced circular dichroism spectrum of 4.7 μM P_2 by DNA at $R = 0.045$ (a) and the corresponding absorption spectrum (right axis) (b) (20 mM phosphate buffer, pH 7.1, 10 mM NaCl).

tetraphenylporphyrin derivatives, the presence of four bulky cationic *meso*-substituents causes strong affinity of P_1 to the negatively charged phosphate backbone while preventing the *meso*-phenyl moieties of P_1 from intercalating between the base pairs.

The efficiency of FRET between excited nucleic acids and the bound P_1 suggests a close placement of the porphyrin units and the corresponding nucleobase donors. The number of covered base pairs by P_1 is 8.6, which is in agreement with reported values for outside-bound tetratolylporphyrins. This differs significantly from the exclusion parameter of intercalating porphyrins (e.g., the value of 2.7 estimated for TMPyP[20]).

E. Binding of Porphyrin Aggregates to Nucleic Acids. The porphyrin P_1 is predominantly monomeric in aqueous solutions, the porphyrin P_2 consists of a mixture of the monomer and aggregates, and the porphyrins P_3 and P_4 form extended aggregates. As expected, aggregation considerably affects the interaction of P_2–P_4 with nucleic acids.

The DNA binding experiments were particularly interesting with P_2. The UV/vis (Figure 8b), RLS (Figure 3), and CD (Figure 8a) spectra depend on the porphyrin/DNA molar ratio R. The binding of the P_2 monomer to DNA is evidenced by a red shift of the absorption band from 416 to 423 nm. The monomer and aggregates are achiral and have no CD spectra. However, in the presence of DNA, an induced CD spectrum of bound P_2 appears (Figure 8a), which consists of an intense bisignate signal with a positive peak at 438 nm and a negative peak at 467 nm, with the total intensity of both bands at $\Delta\epsilon \approx$ |96| M^{-1} cm^{-1}. The zero cross point at 442 nm is very close to the position of the absorption band of J-aggregates at 443–446 nm (Figure 8b). The resolution of the spectra indicated a dominant contribution of a conservative spectrum of equal but opposite rotatory strengths, and a contribution of a small positive peak centered at about 422 nm. From a comparison with the corresponding absorption spectrum (Figure 8b), the conservative signal can be assigned to exciton splitting within the bound assemblies that are characterized by the absorption peak at 443–446 nm. The 422 nm band in the CD spectrum corresponds to the bound monomer with the absorption peak at 423 nm. An induced positive CD band at 389 nm is coincident with the absorption band at 389 nm previously assigned to the H-type aggregates of P_2.

The RLS spectra of P_2 at low R (Figure 3) show light-scattering peaks at 389 and 454 nm having the same intensity level as in the DNA-free solutions. At $R > 0.1$, the absorption band of the bound monomer at 423 nm is broadened and the band of the aggregates at 446 nm becomes dominant. This is accompanied by more than a 2-fold increase in the intensity of the RLS bands of the aggregates at 389 and 454 nm, respectively, compared to that of the DNA-free solutions (Figure 3). These data indicate that the nucleic acid backbone serves as a

chiral template for both externally bound individual porphyrin molecules and different types of extended assemblies. At $R < 0.06$, the monomer and aggregates originally present in the solution independently deposit on the surface of DNA. At higher R, the size of the porphyrin-based assemblies deposited on the DNA surface increases compared to that of the assemblies in solution.

In contrast to P_1 and P_2, the porphyrins P_3 and P_4 are bound predominantly in the form of extended assemblies on the nucleic acid's surface.[20,46] The extended assemblies of P_3 and P_4 behave similarly to P_2 regardless of the nucleic acid sequence.

One would expect that the Coulombic attraction between porphyrin phosphonium groups and a negatively charged sugar–phosphate DNA backbone is stronger than π–π stacking interaction between porphyrin units, and that the binding would lead to the deaggregation of porphyrin assemblies. We have not found any evidence of the deaggregation behavior within 24 h after addition of DNA, possibly because the porphyrin aggregates deposited on the surface of nucleic acids are stabilized by hydrophobic interactions between the porphyrin units, thus minimizing interaction of the porphyrins with polar solvent molecules. The alkyl/aryl substituents of phosphonium groups, negative counterions, and polar solvent provide a very efficient screening of the anionic DNA surface. The free energy gain due to a reorganization of water molecules around the ionic groups can even stabilize close contacts of two groups bearing the same charge.[47]

F. Triplet States of the Porphyrins Bound to Nucleic Acids. Photophysical properties of porphyrins P_1–P_4 depend dramatically on the aggregation state. Aggregates show more than 1 order of magnitude lower quantum yields of the triplet states, which is caused by the fast competitive nonradiative transitions.[48] Here, we report on the rate constant k_T of a triplet state deactivation by dissolved oxygen of the P_1 monomer and compare it with those of the P_1 monomer bound to monophosphates, oligonucleotides, and DNA. Similarly, the formation of singlet oxygen generated by the P_1 triplet states was studied in the presence and absence of DNA. The rate constants k_T of the bound P_1, indicating a profound increase in triplet-state lifetimes ($1/k_T$) upon binding to the nucleic acid's matrix, are presented in Table 1. In some cases the decay curves of the triplet state showed a biphasic behavior, and the rate constant of the faster process was coincident with the k_T value of the free porphyrin. The ratio of free to bound P_1 in the triplet states was obtained by biexponential fitting of the decay curves. We found that the contribution of each form did not match the molar ratio of free to bound P_1 in the ground state calculated using the binding constants in Table 1. For example, triplet quenching measurements suggest that even at a 70-fold excess of DNA about 20% of all P_1 in the triplet states was not bound to DNA (independently of the excitation energy over the range of 50 μJ to 3 mJ), while the ground-state absorption spectra indicate a complete binding (no change upon further addition of DNA). This discrepancy can be explained by dissociation of bound P_1 during the lifetime of the excited states.

Singlet oxygen O$_2$($^1\Delta_g$) is formed by quenching the triplet states of free and bound P_1 monomers by dissolved oxygen (Figure 9). The decay curves of O$_2$($^1\Delta_g$) are governed by the kinetics of quenching of the triplet states characterized by the k_T value. Therefore, singlet oxygen is formed much more slowly with bound P_1 compared to unbound P_1 (Figure 9a,b). The same amplitudes of the singlet oxygen signals of P_1 and P_1 bound to DNA indicate that the quantum yields of singlet oxygen formation remain unchanged by the binding. The O$_2$($^1\Delta_g$)
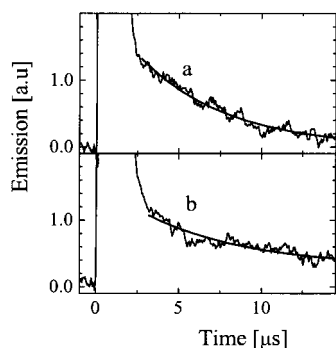
Preprogramming of Porphyrin−Nucleic Acid Assemblies

J. Phys. Chem. B, Vol. 106, No. 26, 2002 **6791**

Figure 9. Singlet oxygen phosphorescence at 1270 nm: 1.7 μM P_1 (λ_{exc} = 416 nm) (a) and 1.7 μM P_1 in the presence of DNA (R = 0.029, λ_{exc} = 422 nm) (b). The smooth line is a least-squares fit to the monoexponential function. Each trace is an average from 500 traces. Singlet oxygen was generated by a 28 ns laser pulse (700 μJ/pulse) in air-saturated 20 mM phosphate buffer, pH 7.0, 100 mM NaCl. The strong red emission at the beginning of the trace (0−3 μs) is due to fluorescence of the sample.

lifetime in oxygen-saturated solution was estimated to be ~2 μs, which is in agreement with previously published values for singlet oxygen in aqueous solutions.[49]

4. Conclusion

The present study shows that the selection of substituents of the porphyrin macrocycle allows us to preprogram the behavior of the porphyrins in aqueous solutions. It is shown here that the phosphonium moiety offers the possibility of controlling the aggregation of the porphyrin derivatives via a delicate balance between steric requirements and hydrophobicity of the alkyl/aryl substituents attached to the phosphorus atom. The relatively small changes in the character of the phosphonium moieties have dramatic effects on the aggregation and photophysical properties of the porphyrins. The porphyrin P_1 shows a strong tendency toward a monomeric state, while the porphyrin P_2 is present in solution with an equilibrium of the monomer and aggregated states. The porphyrins P_3 and P_4 are almost solely present in the form of extended aggregates.

It was demonstrated that the stacking interaction between porphyrin units (cofacial aggregates) and the hydrophobic interactions between alkyl/aryl residues of the phosphonium moieties and the porphyrin macrocycles stabilize the aggregated forms. Such stabilization of the aggregates is stronger than Coulombic attraction between the positively charged phosphonium moieties and the phosphate backbone of nucleic acids. The direct result of this behavior is that the porphyrin derivatives are deposited on the DNA surface in the same form as they were in solution. This behavior was observed for various conditions, including relatively high DNA concentration (R < 1) and ionic strength (0.1 M NaCl). The structure and the type of the respective porphyrin−nucleic acid complexes and assemblies were characterized by various spectroscopic techniques.

References and Notes

(1) Alberts, B.; Bray, D.; Lewis, J.; Raff, M.; Roberts, K.; Watson, J. D. *Molecular Biology of The Cell*; Garland Publishing: New York, London, 1994.

(2) (a) Cohen, S. M.; Lippard, S. J. *Prog. Nucleic Acid Res. Mol. Biol.* **2001**, *67*, 93. (b) De Clercq, E. *Pure Appl. Chem.* **2001**, *73*, 55. (c) De Clercq, E. *Rev. Med. Virol.* **2000**, *10*, 255. (c) *DNA and RNA Cleavers and Chemotherapy of Cancer and Viral Diseases*; Meunier, B., Ed.; NATO ASI Series, Series C; Kluwer: Dordrecht, The Netherlands, 1996; p 479. (d) Lippert, B. *BioMetals* **1992**, *5*, 195.

(3) (a) Macdonald, I. J.; Dougherty, T. J. *J. Porphyrins Phthalocyanines* **2001**, *5*, 105. (b) Bonnett, R. *Chemical Aspects of Photodynamic Therapy*; G & B Science: London, 2000. (c) Henderson, B. W.; Dougherty, T. J. *Photodynamic Therapy*; Marcel Dekker: New York, 1992.

(4) (a) Asanaka, M.; Kurimura, T.; Toya, H.; Ogaki, J.; Kato, Y. *AIDS (London)* **1989**, *3*, 403. (b) Dixon, D. W.; Marzilli, L. G.; Schinazi, R. *Ann. N.Y. Acad. Sci.* **1990**, *616*, 511. (c) Sessler, J. L.; Cyr, M. J.; Maiya, B. G.; Judy, M.; Newman, J. T.; Skiles, H. L.; Boriak, R.; Matthews, J. L.; Chanh, T. C. *Proc. SPIE-Int. Opt. Eng.* **1990**, *1203*, 233. (d) Levere, R. D.; Gong, Y. F.; Kappas, A.; Bucher, D. J.; Womser, G. P.; Abraham, N. G. *Proc. Natl. Acad. Sci. U.S.A.* **1991**, *88*, 1756. (e) Debnath, A. K.; Jiang, S.; Strick, N.; Haberfield, P.; Neurath, R. A. *J. Med. Chem.* **1994**, *37*, 1099.

(5) Arthanari, H.; Basu, S.; Kawano, T. L.; Bolton, P. H. *Nucleic Acids Res.* **1998**, *26*, 3724.

(6) (a) Bigey, P.; Soennichsen, S. H.; Meunier, B.; Nielsen, P. E. *Bioconjugate Chem.* **1997**, *8*, 267. (b) Mestre, B.; Pitie, M.; Loup, C.; Claparols, C.; Pratviel, G.; Meunier, B. *Nucleic Acids Res.* **1997**, *25*, 1022. (c) Li, H.; Fedorova, O. S.; Trumble, W. R.; Fletcher, T.; Czuchajowski, L. *Bioconjugate Chem.* **1997**, *8*, 49. (d) Mettath, S.; Munson, B. R.; Pandey, R. K. *Bioconjugate Chem.* **1999**, *10*, 94. (e) Berlin, K.; Jain, R. K.; Simon, M. D.; Richert, C. *J. Org. Chem.* **1998**, *63*, 1527. (f) Tabata, M.; Sarker, A. K.; Watanabe, K. *Chem. Lett.* **1998**, 325.

(7) Dabrowiak, J. C.; Ward, B.; Goodisman, J. *Biochemistry* **1989**, *28*, 3313.

(8) Wheelhouse, R. T.; Sun, D.; Han, H.; Han, F. X.; Hurley, L. H. *J. Am. Chem. Soc.* **1998**, *120*, 3261.

(9) Uno, T.; Hamasaki, K.; Tanigawa, M.; Shimbayashi, S. *Inorg. Chem.* **1997**, *36*, 1676.

(10) Lauceri, R.; Campagna, T.; Contino, A.; Purrello, R. *Angew. Chem., Int. Ed. Engl.* **1996**, *35*, 215.

(11) Anantha, N. V.; Azam, M.; Sheardy, R. D. *Biochemistry* **1998**, *37*, 2709.

(12) (a) Lugo-Ponce, P.; McMillin, D. R. *Coord. Chem. Rev.* **2001**, *208*, 169. (b) Eggleston, M. K.; Crites, D. K.; McMillin, D. R. *J. Phys. Chem. A* **1998**, *102*, 5506.

(13) (a) Wall, R. K.; Shelton, A. H.; Bonaccorsi, L. C.; Bejune, S. A.; Dube, D.; McMillin, D. R. *J. Am. Chem. Soc.* **2001**, *123*, 11480. (b) Barnes, N. R.; Schreiner, A. F. *Inorg. Chem.* **1998**, *37*, 6935. (c) Fiel, R. J.; Howard, J. C.; Mark, E. H.; Datta Gupta, N. *Nucl. Acids Res.* **1979**, *6*, 3093.

(14) Arthanari, H.; Basu, S.; Kawano, T. L.; Bolton, P. H. *Nucleic Acids Res.* **1998**, *26*, 3724.

(15) (a) Fleischer, E. B. *Inorg. Chem.* **1962**, *1*, 493. (b) Wynter, C. I.; Hambright, P.; Cheek, C. H. *Nature* **1967**, *216*, 1105. (c) Hambright, P.; Fleischer, E. B. *Inorg. Chem.* **1970**, *9*, 1757.

(16) Krishnamurthy, M. *Indian J. Chem.* **1977**, *15B*, 964.

(17) Robic, N.; Bied-Charreton, C.; Perrée-Fauvet, M.; Verchère-Béaur, C.; Salmon, L.; Gaudemer, A.; Pasternack, R. F. *Tetrahedron Lett.* **1990**, *31*, 4739.

(18) (a) Salehi, A.; Mei, H. Y.; Briuce, T. *Tetrahedron Lett.* **1991**, *32*, 3453. Perrée-Fauvet, M.; Gresh, N. *Tetrahedron Lett.* **1995**, *36*, 4227.

(19) Jin, R.; Aoki, S.; Shima, K. *J. Chem. Soc., Faraday Trans.* **1997**, *93*, 3945.

(20) Kubát, P.; Lang, K.; Anzenbacher, P., Jr.; Král, V.; Ehrenberg, B. *J. Chem. Soc., Perkin Trans. 1* **2000**, 933.

(21) (a) Fiel, R. J.; Howard, J. C.; Mark, E. H.; Datta-Gupta, N. *Nucleic Acids Res.* **1979**, *6*, 3039. (b) Musser, D. A.; Datta-Gupta, N.; Fiel, R. J. *Biochem. Biophys. Res. Commun.* **1980**, *97*, 918. (c) Carvlin, M. J.; Datta-Gupta, N.; Fiel, R. J. *Biochem. Biophys. Res. Commun.* **1982**, *108*, 66. (d) Fiel, R. J.; Beerman, T. A.; Mark, E. H.; Datta-Gupta, N. *Biochem. Biophys. Res. Commun.* **1982**, *108*, 1067.

(22) Mukundan, N. E.; Petho, G.; Dixon, D. W.; Kim, M. S.; Marzilli, L. G. *Inorg. Chem.* **1994**, *33*, 4676.

(23) Pasternack, R. F.; Gibs, E. J.; Villafranca, J. J. *Biochemistry* **1983**, *22*, 2406.

(24) Vergeldt, F. J.; Koehorst, R. B. M.; van Hoek, A.; Schaafsma, T. J. *J. Phys. Chem.* **1995**, *99*, 4397.

(25) (a) Pasternack, R. F.; Gibs, E. J. In *Metal Ions in Biological Systems*; Sigel, A., Sigel, H., Eds.; Marcel Dekker: New York, 1996; Vol. 33, Chapter 12. (b) Marzilli, L. G.; Banville, D. L.; Zon, G.; Wilson, W. D. *J. Am. Chem. Soc.* **1986**, *108*, 4188. (c) Lipscomb, L. A.; Zhou, F. X.; Presnell, S. R.; Woo, R. J.; Peek, M. E.; Plaskon, R. R.; Williams, L. D. *Biochemistry* **1996**, *35*, 2818. (d) Mukundan, N. E.; Petho, G.; Dixon, D. W.; Kim, M. S.; Marzilli, L. G. *Inorg. Chem.* **1994**, *33*, 4676.

(26) Khairutdinov, R. F.; Serpone, N. *J. Phys. Chem. B* **1999**, *103*, 761.

(27) (a) Meunier, B. *Chem. Rev.* **1992**, *92*, 141. (b) Knapp Pogozelski, W.; Tullius, T. D. *Chem. Rev.* **1998**, *98*, 1089. (c) Burrows, C. J.; Muller, J. G. *Chem. Rev.* **1998**, *98*, 1109. (d) Armitage, B. *Chem. Rev.* **1998**, *98*, 1171.

(28) From a design perspective, these porphyrins are expected to display Φ_T and Φ_Δ similar to those of *meso*-tetraphenylporphyrin (TPP), and also to be water-soluble and exhibit binding affinities for DNA augmented by the positively charged substituents.

(29) Wells, R.; Larson, J. E.; Grant, R. C.; Shortle, B. E.; Cantor, C. R. *J. Mol. Biol.* **1970**, *54*, 465.

(30) Wen, L.; Li, M.; Schlenoff, J. B. *J. Am. Chem. Soc.* **1997**, *119*, 7726.

(31) Jasuja, R.; Jameson, D. M.; Nashijo, C. K.; Larsen, R. W. *J. Phys. Chem. B* **1997**, *101*, 1444.

(32) Bevington, P. R. *Data Reduction and Error Analysis for the Physical Sciences*; McGraw-Hill: New York, 1969.

(33) McGhee, J. D.; von Hippel, P. H. *J. Mol. Biol.* **1974**, *86*, 469.

(34) Gardecki, J. A.; Maroncelli, M. *Appl. Spectrosc.* **1998**, *52*, 1179.

(35) Gensch, T.; Braslavsky, S. E. *J. Phys. Chem. B* **1997**, *101*, 101.

(36) Lang, K.; Anzenbacher, P., Jr.; Kapusta, P.; Král, V.; Kubát, P.; Wagnerová, D. M. *J. Photochem. Photobiol., B* **2000**, *57*, 51.

(37) (a) Pasternack, R. F.; Collings, P. J. *Science* **1995**, *369*, 935. (b) de Paula, C. C.; Robblee, J. H.; Pasternack, R. F. *Biophys. J.* **1995**, *68*, 335.

(38) Kano, K.; Fukuda, K.; Wakami, H.; Nishiabu, R.; Pasternack, R. F. *J. Am. Chem. Soc.* **2000**, *122*, 7494.

(39) Hunter, C. A.; Sanders, J. K. M. *J. Am. Chem. Soc.* **1990**, *112*, 5525.

(40) (a) Kasha, M.; Rawls, H. R.; El Bayoumi, A. *Pure Appl. Chem.* **1965**, *11*, 371. (b) *J-aggregates*; Kobayashi, T., Ed.; World Scientific: Singapore, 1996. (c) Micali, N.; Romeo, A.; Lauceri, R.; Purrello, R.; Mallamace, F.; Scolaro, L. M. *J. Phys. Chem. B* **2000**, *104*, 9416.

(41) Sirish, M.; Schneider, H.-J. *Chem. Commun.* **2000**, 23.

(42) Pasternack, R. F.; Gibbs, E. J.; Gaudemer, A.; Antebi, A.; Bassner, S.; De Poy, L.; Turner, D. H.; Williams, A.; Laplace, F.; Lansard, M. H.; Merienne, C.; Perrée-Fauvet, M. *J. Am. Chem. Soc.* **1985**, *107*, 8179.

(43) The intercalation of porphyrin between nucleobases can be almost totally excluded as it is typically accompanied by a large red shift of the Soret band (more than 8 nm) with substantial hypochromism and by negative signals in induced CD spectra. For reference see: Mukundan, N. E.; Petho, G.; Dixon, D. W.; Kim, M. S.; Marzilli, L. G. *Inorg. Chem.* **1994**, *33*, 4676, and Huang, X. F.; Nakanishi, K.; Berova, N. *Chirality* **2000**, *12*, 237.

(44) Sehlstedt, U.; Kim, S. K.; Carter, P.; Goodisman, J.; Vollano, J. F.; Norden, B.; Dabroviak, J. C. *Biochemistry* **1994**, *33*, 41.

(45) Similar experiments were also performed with CMP. The absorption band of CMP in the region 250−300 nm was adjusted to the same value as for solutions of oligonucleotides. Under these conditions the concentration of CMP is up to 40 μM; i.e., it is too low to form any adduct with $\mathbf{P}_1$ since the corresponding K_b is only 15 M^{-1} (Table 1). Here the presence of optically matched CMP at 271 nm decreases the fluorescence emission of $\mathbf{P}_1$ by a factor of 1.5 related to $\mathbf{P}_1$ in the absence of CMP. This indicates that there is no energy transfer between free porphyrin and free nucleotide in the solution and only the inner filter effect takes place.

(46) (a) Toma, H. E.; Araki, K. *Coord. Chem. Rev.* **2000**, *196*, 307. (b) Yun, B. H.; Jeon, S. H.; Cho, T. S.; Yi, S. Y.; Sehlsted, U.; Kim, S. K. *Biophys. Chem.* **1998**, *70*, 1.

(47) (a) No, K. T.; Nam, K.-Y.; Scheraga, H. A. *J. Am. Chem. Soc.* **1997**, *119*, 12917. (b) Šponer, J.; Šponer, J. E.; Gorb, L.; Leszczynski, J.; Lippert, B. *J. Phys. Chem. B* **1999**, *103*, 11406.

(48) Richelli, F. *J. Photochem. Photobiol. B* **1995**, *29*, 109.

(49) Wilkinson, F.; Helman, P.; Ross, A. B. *J. Phys. Chem. Ref. Data* **1995**, *24*, 663.